

## LOW-TEMPERATURE STERILIZATION INFLUENCE ON FUSED DEPOSITION MODELLING PARTS

Diana POPESCU<sup>1,\*</sup>, Daniel VLĂSCEANU<sup>2</sup>, Lucian CURSARU<sup>3</sup>, Florin BACIU<sup>4</sup>, Anton HADAR<sup>5,6</sup>

<sup>1)</sup> Assoc. Prof., PhD, Department of Machine and Production System, University "Politehnica" of Bucharest, Bucharest, Romania

<sup>2)</sup> Lecturer, PhD, Department of Strength Materials, University "Politehnica" of Bucharest, Romania

<sup>3)</sup> Master student, University "Politehnica" of Bucharest, Eng., Top Metrology SA

<sup>4)</sup> Lecturer, PhD, Department of Strength Materials, University "Politehnica" of Bucharest, Romania

<sup>5)</sup> Prof., PhD, Department of Strength Materials, University "Politehnica" of Bucharest, Romania

<sup>6)</sup> Romanian Academy of Science

**Abstract:** Fused Deposition Modelling (FDM) along with other Additive Manufacturing (AM) processes are used today in a large number of applications among which those dedicated to the medical field are focused on manufacturing anatomical models, surgical devices, implants or prostheses. While anatomical models are mainly manufactured for patient communication, visualization, surgery training, rehearsal or simulation, there are also 3D printed medical objects that come in contact with the patient body tissues and fluids. Therefore, in their case sterilization and biocompatibility testing are mandatory steps before use. In this context, the current paper is studying the influence of sterilization on the compressive strength of FDM objects, as well as on their dimensional accuracy. Standard samples for evaluating the compressive strength of FDM objects manufactured from ABS (Acrylonitrile-butadiene-styrene) material were used. For assessing the dimensional accuracy, a test part was designed, manufactured and sterilized. The test part was measured before and after sterilization, a comparison with the virtual part being made. The results of this study can be used by designers as they provide valuable information on how to design 3D printed parts.

**Key words:** Fused Deposition Modelling, medical applications, sterilization, compressive strength, dimensional accuracy.

### 1. INTRODUCTION

The key advantages offered by Additive Manufacturing (AM) technology in the medical field are: high geometrical complexity of fabricated parts, cost efficiency in case of manufacturing prototypes or small batches of parts, easy product customization based on patient anatomical data and needs, and direct fabrication of parts from their three-dimensional virtual model without requiring the design and use of tooling, gauges or fixtures [1]. Also, AM capability to build porous structures, multi-materials parts or open-cellular foams make this technology appropriate for tissue engineering applications [2].

AM limitations are related mostly to the still limited range of usable materials. Moreover, the mechanical properties, surface finish and accuracy of AM parts could be inferior to those machined or moulded, therefore suitable only for some categories of medical devices [3].

AM technology is used in medical field [4] for building: anatomical models (for visualization, preoperative planning, surgery simulations and/or rehearsal, medical education and training, patient-doctor communication), medical devices used intra-operative (patient-specific guides, customized devices and surgical tools), implants and prostheses, and organs or tissue printing (currently in the research & development stage).

Along Stereolithography, Laser Sintering and Melting processes, Fused Deposition Modeling (FDM) is one of the AM processes quite often used in medical applications. In FDM, ABS (Acrylonitrile-butadiene-styrene) or PLA (Polylactic acid) filaments of materials are extruded through a nozzle (or two nozzles for some FDM machines) and deposited for forming each layer of material. These layers are successively added one of the top of the other until the whole part is built. The nozzles' deposition paths are generated by the machine's software after slicing the 3D virtual model of the part. For applications in which the devices are customized according to the patient anatomy, medical scanning data: Computer Tomography (CT) or MRI (Magnetic Resonance Imaging) can be used.

#### 1.1. Problem statement

In medical applications where the 3D-printed objects come in contact with patient body tissues and fluids, it is mandatory to use materials which can be sterilized and/or are biocompatible. Moreover, as sterilization process is

\* Corresponding author: University "Politehnica" of Bucharest, Department of Machine and Production Systems, Splaiul Independentei, 313, sector 6, Bucharest, Romania,  
Tel.: 0040214029759;  
Fax: 0040214029759;  
E-mail addresses: [diana@mix.mmi.pub.ro](mailto:diana@mix.mmi.pub.ro) (D. Popescu),  
[daniel.vlasceanu@upb.ro](mailto:daniel.vlasceanu@upb.ro) (D. Vlasceanu),  
[lucian.cursaru@topmetrology.ro](mailto:lucian.cursaru@topmetrology.ro) (L. Cursaru),  
[anton.hadar@upb.ro](mailto:anton.hadar@upb.ro) (A. Hadar),  
[florin.baciu@upb.ro](mailto:florin.baciu@upb.ro) (F. Baciu).

taking place at a temperature higher than 60°C, the temperature influence over the mechanical and geometrical properties of plastic medical devices should be investigated and known before their design, manufacturing and use.

In this context, this paper is studying the influence of low-temperature gas plasma sterilization process on the mechanical properties (more exactly, on the compressive strength) of ABS FDM parts and on their dimensional accuracy. The research results are useful for designers in knowing whether or not certain features are sterilization-stable. And thus, the designers can properly adapt the design of devices to the medical application specific constraints. A test part containing different types of geometric features placed in diverse positions/orientations, having small to medium dimensions was modeled and manufactured. Using an industrial CT system, the test part was measured before and after sterilization and the reconstructed virtual parts were compared with the virtual part.

## 1.2. Literature review

Literature survey showed a small number of independent researches on this subject. In the majority of applications, information provided by AM material producers are employed [5–6], medical grade resins, powders or filaments usually being recommended for use.

There are several types of sterilization processes: gamma irradiation, electron beam irradiation, gas plasma, X-ray or ethylene oxide gas sterilization, steam or dry heat sterilization. Each of them has advantages and disadvantages, and influences differently the sterilized object. Reports are showing modifications in color, odor or mechanical properties (strength or rigidity).

Perez et al. [7] studied the influence of five different sterilization techniques over the mechanical behavior of standard test parts manufactured from nine FDM materials. Sterility testing was also performed for each material and sterilization method. The results showed that low-temperature sterilization methods are not determining significant mechanical damages over the plastic FDM parts, in the same time ensuring the required sterility conditions. The compressive and tensile strength of sterilized FDM parts were not analyzed in this paper.

Sterilization process was investigated also in [8] for determining if sterile parts can be built from a non-sterile filament of PLA material. The interest for this type of material is given by its extensive use in FDM process by the low-cost 3D printers. The results showed not only that PLA parts can be sterilized, but also that the 3D printed process can produce itself, due to the high processing temperature, sterile parts.

Fürnstahl et al. [9] analyzed the deformation of a test model surgical guide after steam pressure sterilization for two types of materials: PA 2200 (Selective Laser Sintering process) and VisiJet Chrystal (for jet-printing processes). The maximum measured error was 0.5 mm for thin wall cylinders. The authors suggested, as design rule, not to prescribe walls with less than 1 mm thickness if steam pressure is applied as sterilization method.

Although the mechanical properties of FDM parts were investigated for different parameter settings and for

different building orientation [10–13], to the best of our knowledge, no data are available regarding the effect of low-temperature sterilization over the compressive strength of ABS parts manufactured using FDM process.

## 2. MATERIALS AND METHOD

### 2.1. Test part design

*Test part for compression testing.* Cylindrical test parts (20 mm diameter, 20 mm height) were built of ABS material on Mojo 3D Printer (Stratasys Inc.), in two orientations (with cylinders axis along and perpendicular on the building direction –  $z$  axis) using a slice height of 0.178 mm.

*Geometric benchmark part.* Test parts developed by different researchers [14–15] usually include multiple features representing certain geometrical characteristics. These features have various sizes, are differently oriented relative to the direction of build and are placed in diverse positions relative to the AM machine workspace. Their main function is to allow the evaluation of one or more characteristics: geometrical dimensioning and tolerancing (GD&T), repeatability, surface quality, capability to manufacture thin walls or overhang features, spherical or freeform surfaces, slopes of different angles, capability to manufacture small sizes features, etc. These parts are called geometric test parts and are used to "evaluate the geometrical quality of the features generated by a certain machine" [16].

There are also test parts developed for assessing "the mechanical properties of features or geometries generated by a certain AM machine" [16] – called mechanical benchmark parts, as there are test parts manufactured by varying the process parameters (layer style building, process parameters settings, building orientation, etc.), designed to improve existing processes or to allow the characterization and testing of new AM materials – which are called process test parts.

In this study, a geometrical benchmark part was designed (100 mm × 100 mm × 32 mm) so that to include geometrical features such as cylinders, hollow cylinders, slots, thin walls and slope walls, all with small to medium dimensions, usually encountered in the design of surgical guides or other medical devices [17]. Figure 1 presents the virtual test part. Table 1 lists the type and number of features, as well as their nominal dimensions.

This benchmark part was designed not to contain features which need support structures (45° angle rule) and to be easy to measure.

### 2.2. Sterilization process

Test parts manufactured from ABS material were subjected to low-temperature hydrogen peroxide gas plasma sterilization using a Sterrad system from Colentina Clinical Hospital in Bucharest. Autoclave sterilization (also available at Colentina Clinical Hospital in Bucharest) proved an inappropriate solution as high temperature will heavily deform/melt the plastic parts.

The standard cycle for gas plasma sterilization is 55 minutes long and involves wrapping the part in a synthetic package, placing it in a vacuum chamber and bringing to 60°C temperature.

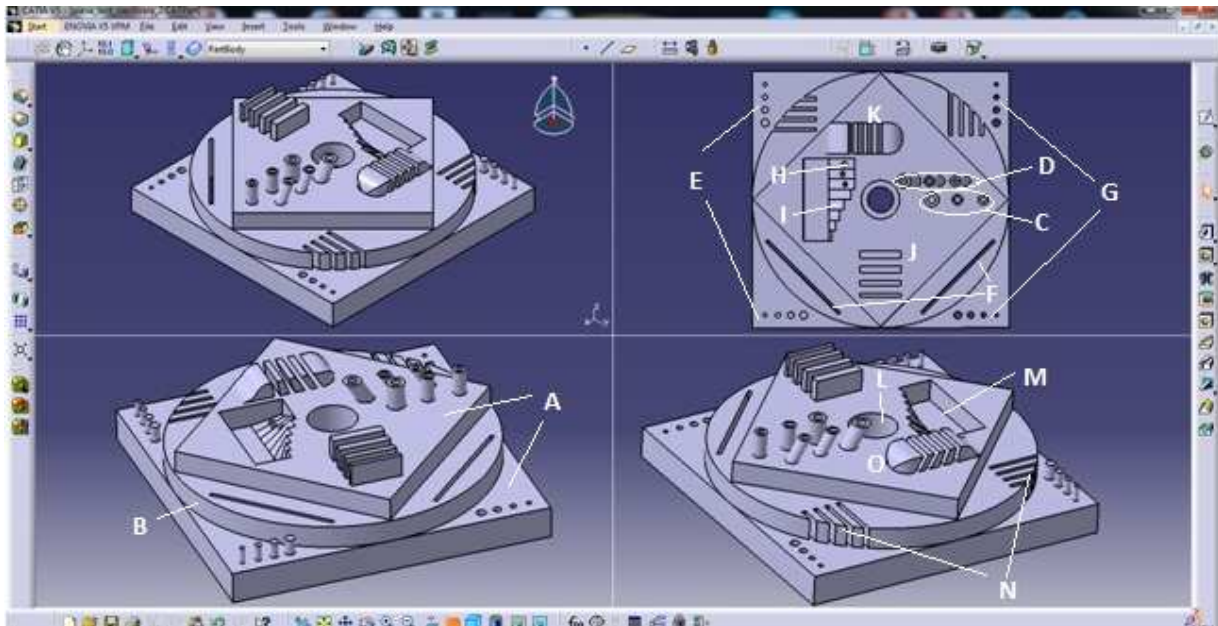


Fig. 1. Geometrical benchmark part.

Table 1

Benchmark part features nominal dimensions

Feature	Number of features	Position	Dimensions
A. Parallelepipeds	2	1 with sides parallel with $x$ and $y$ axes 1 with sides perpendicular on $x$ and $y$ axes	$100\text{ mm} \times 100\text{ mm} \times 10\text{ mm}$ $70\text{ mm} \times 70\text{ mm} \times 7\text{ mm}$
B. Cylinder	1	Vertical axis	$100\text{ mm diameter} \times 7\text{ mm height}$
C. Hollow cylinders	3	Vertical axis, placed along $x$ axis	$D_{\text{ext}} 4\text{ mm}, D_{\text{int}} 2\text{ mm} \times 8\text{ mm height}$ $D_{\text{ext}} 4\text{ mm}, D_{\text{int}} 2.5\text{ mm} \times 8\text{ mm height}$ $D_{\text{ext}} 5.5\text{ mm}, D_{\text{int}} 3\text{ mm} \times 8\text{ mm height}$
D. Inclined hollow cylinders	3	Axis at $60^\circ$ in respect to $xy$ plane	$D_{\text{ext}} 4\text{ mm}, D_{\text{int}} 2\text{ mm} \times 8\text{ mm height}$ $D_{\text{ext}} 4\text{ mm}, D_{\text{int}} 2.5\text{ mm} \times 8\text{ mm height}$ $D_{\text{ext}} 5.5\text{ mm}, D_{\text{int}} 3\text{ mm} \times 8\text{ mm height}$
E. Cylinders	8	4 along $x$ axis 4 along $y$ axis	Diameters $1.5\text{ mm}, 2\text{ mm}, 2.5\text{ mm}, 3\text{ mm} \times 10\text{ mm height}$
F. Slots	2	At $45^\circ$ in respect to $x$ and $y$ axes	$40\text{ mm} \times 1.27\text{ mm} \times 17\text{ mm}$
G. Holes		4 along $x$ axis 4 along $y$ axis	Diameters $1.5\text{ mm}, 2\text{ mm}, 2.5\text{ mm}, 3\text{ mm} \times 5\text{ mm depth}$
H. Inclined holes	3	$80^\circ, 70^\circ, 60^\circ$ (in respect to $xy$ plane)	$2\text{ mm diameter} \times 2\text{ mm depth}$
I. Slope walls (inside)	8	$10^\circ, 20^\circ, 30^\circ, 40^\circ, 50^\circ, 60^\circ, 70^\circ, 80^\circ$ (with respect to $xy$ plane)	$7\text{--}10\text{ mm} \times 4\text{ mm}$
J. Thin walls (outside)	4	With longer side along $x$ axis	$1.5, 2, 2.5, 3\text{ mm} \times 16\text{ mm} \times 7\text{ mm}$
K. Inclined thin walls		With longer side along $y$ axis	$80^\circ, 70^\circ, 60^\circ, 50^\circ \times 2\text{ mm}$ (top side)
L. Central counterbored hole	1	In the center of the part	$10\text{ mm} \times 24\text{ mm}, 15\text{ mm} \times 10\text{ mm}$
M. Pocket		At $45^\circ$ with respect to $x$ and $y$ axes	$7\text{ mm depth}$
N. Thin walls (inside)	8	4 along $x$ axis 4 along $y$ axis	$1.37\text{ mm} \times 7\text{ mm depth}$
O. Round edges	2	Exterior, At $45^\circ$ with respect to $x$ and $y$ axes	$10\text{ mm radius}$

### 2.3. Testing and measurement processes

*Compressive strength testing.* Instron testing equipment up to 100 kN capacity was used in the experiments.

*Dimensional accuracy.* Measurements are made before and after test part (Fig. 6) sterilization using a Nikon XT H 225 - an industrial CT scanner in combination with VG Studio Max software. The following scanning parameters were used: beam energy – 120 kV, beam current – 170  $\mu\text{A}$ , power – 20.4 W.

### 3. RESULTS

Figures 2 and 3 present stress-strain curves for compression stress load for ABS sterilized and non-sterilized parts, with parallel and perpendicular building directions. Figures 4 and 5 present a comparison of compressive strength for parallel and perpendicular samples, sterilized and non-sterilized.

Measurements were performed on part surfaces in order to evaluate the differences from the nominal part. The values in these points are expressed as  $x, y, z$  coordinates along the deviation value which ( $Var$  [mm]). The color code for the deviation is the following: green – if the deviation value is around 0, blue – negative deviation (measured dimensions are smaller than the nominal value) and red – positive deviation (measured dimensions are larger than the nominal value).

Figure 7 is a screenshot from the measurement software showing the measurements taken in a section of the part. Figure 8 presents the *color map* for the non-sterilized test part. Using part sections, the 3D virtual models of the test part before and after sterilization were reconstructed and superposed on the nominal part (Fig. 9). Figure 10 presents an image of the measurement process on the Nikon CT scanner.

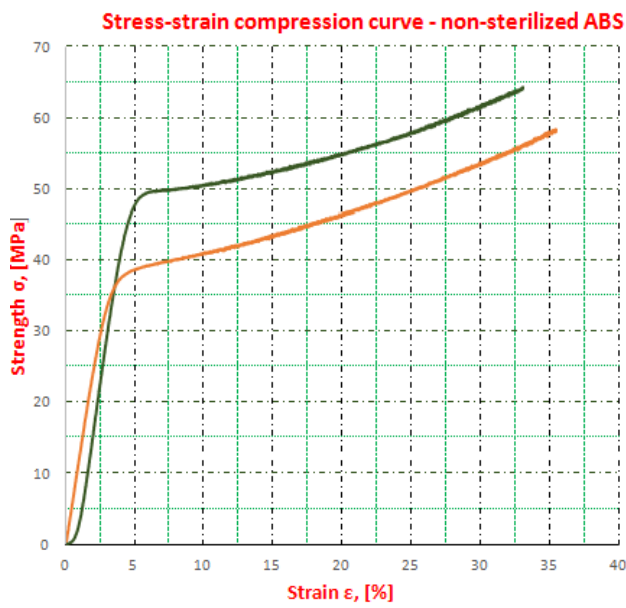


Fig. 2. Stress-strain curve for non-sterilized ABS sample (green– ABS perpendicular, red – ABS parallel).

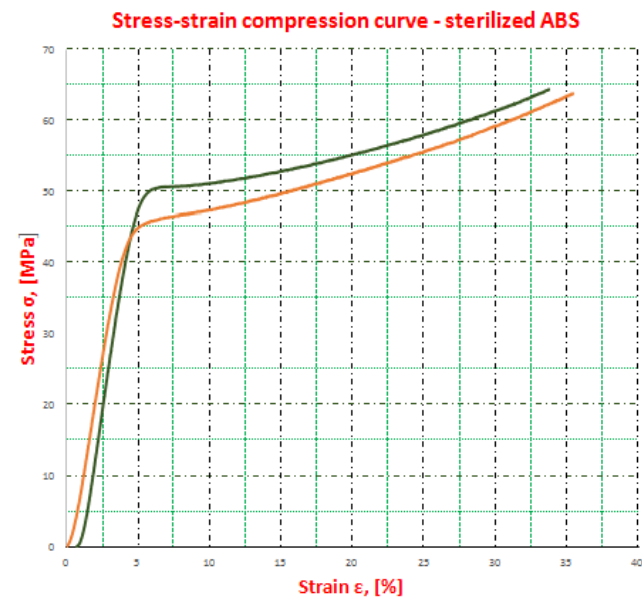


Fig. 3. Stress-strain curve for sterilized ABS sample (green– ABS perpendicular sample, red – ABS parallel sample).

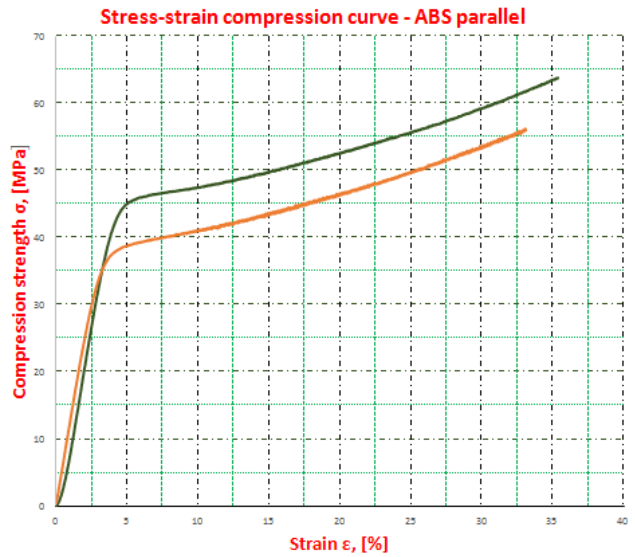


Fig. 4. Stress-strain curve for ABS parallel sample (green– sterilized ABS, red – non-sterilized ABS).

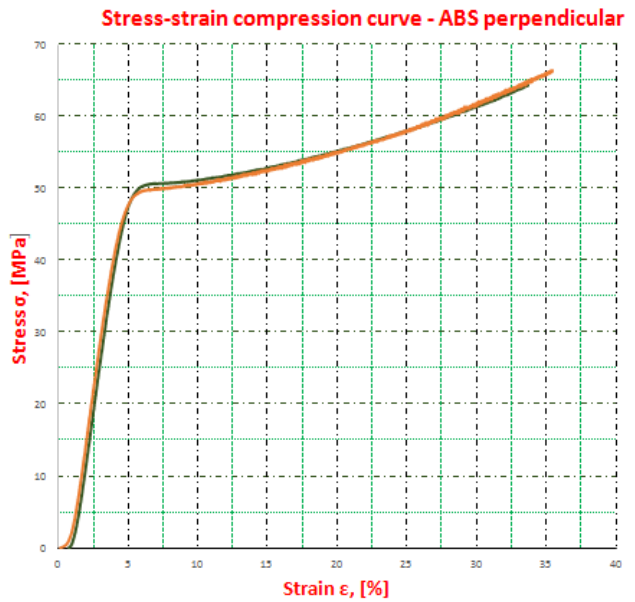


Fig. 5. Stress-strain curve for ABS perpendicular sample (green– sterilized ABS, red – non-sterilized ABS).

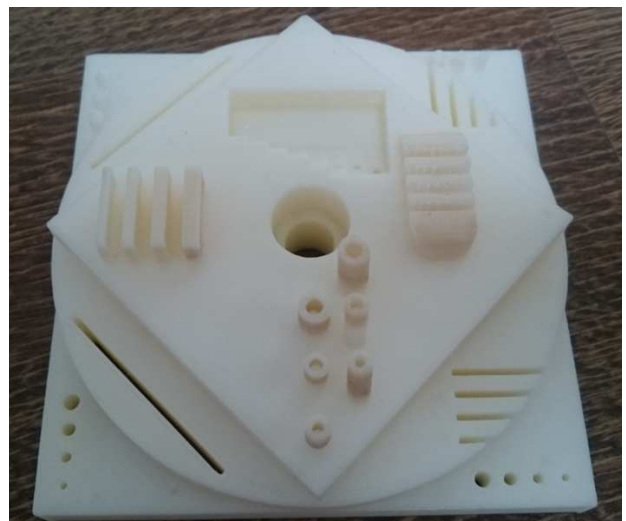


Fig. 6. 3D printed test part.

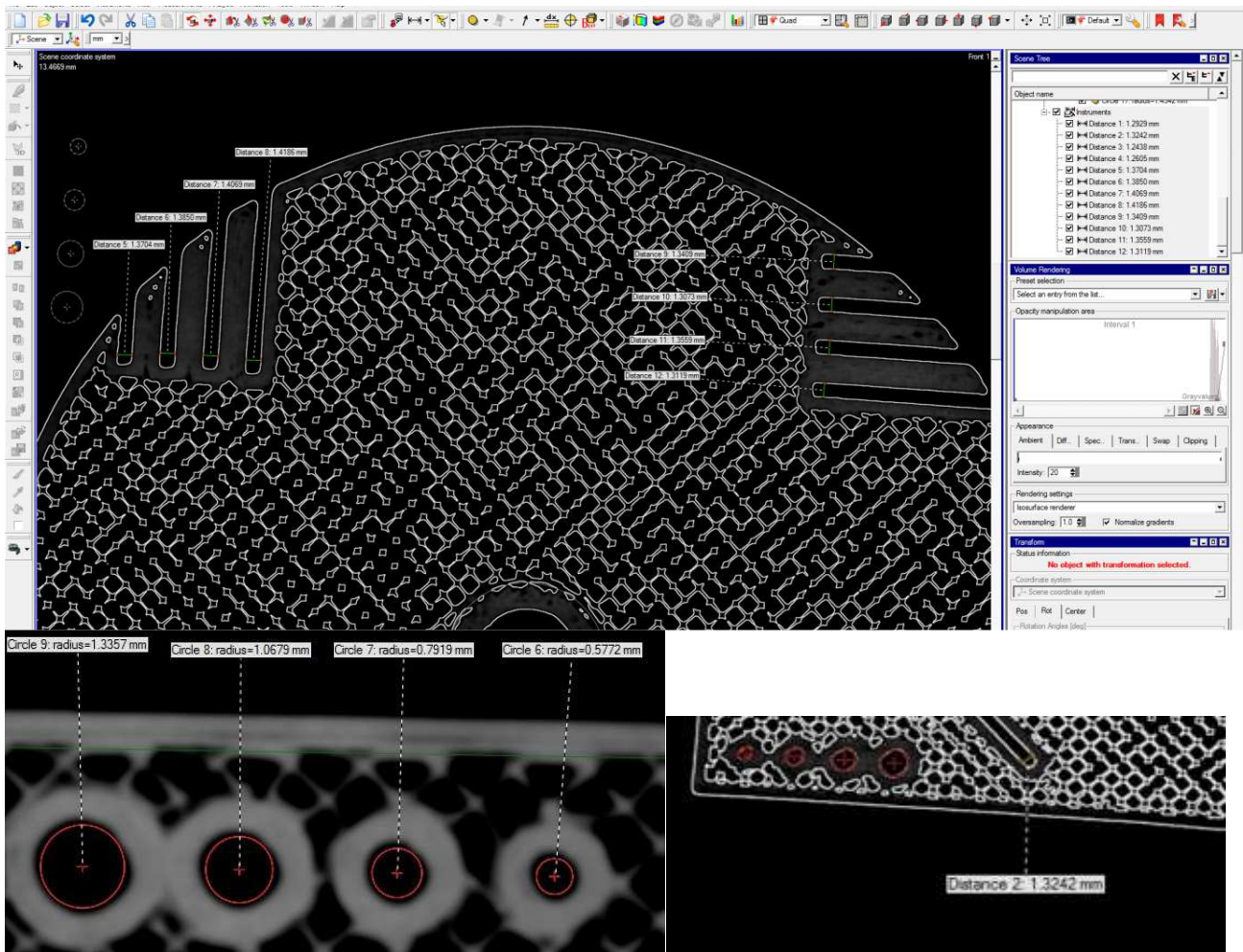


Fig. 7. Screenshots with measurements in three sections of the test part before sterilization.

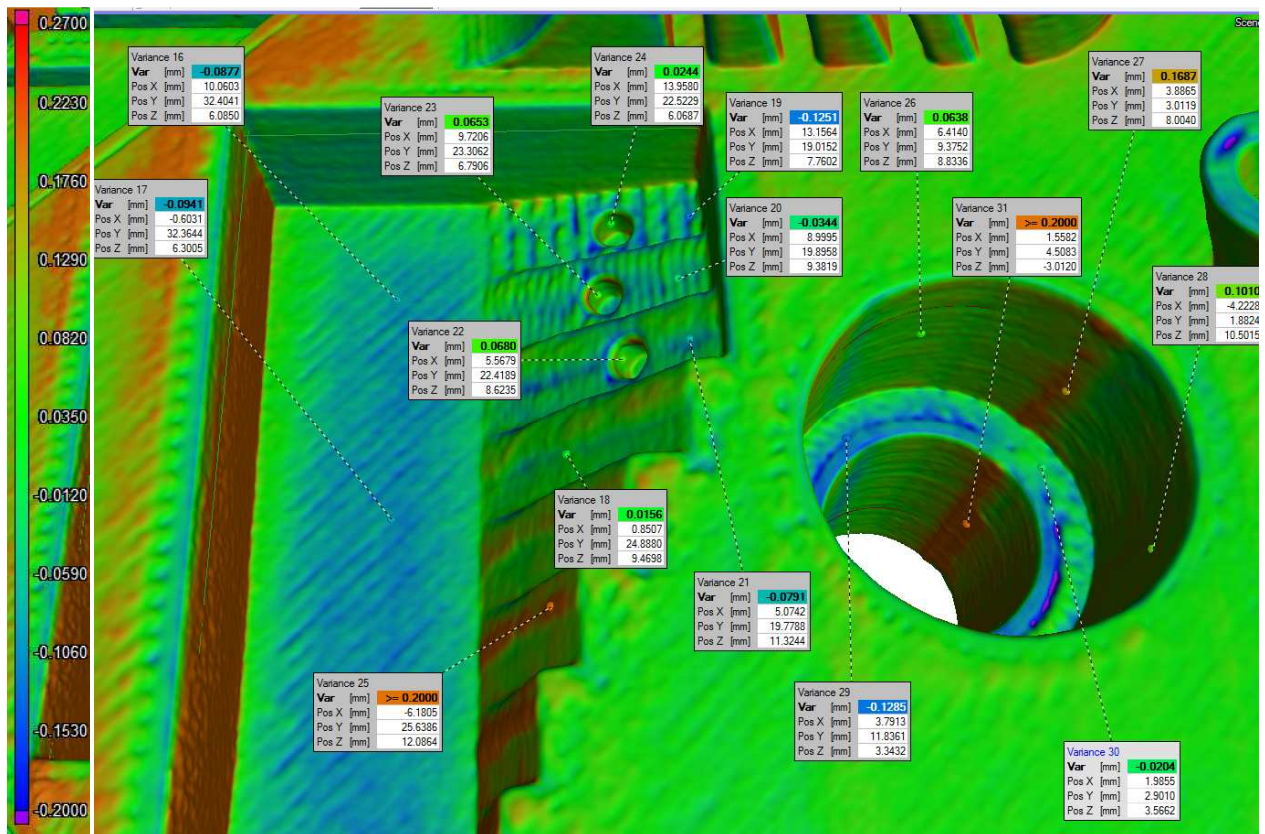


Fig. 8. Color map illustrating the deviation of the test part dimensions from the nominal part.



Fig. 9. Nikon industrial CT scanner.

#### 4. DISCUSSIONS

*Compressive strength.* Based on test results, the compressive strength of ABS parts was calculated in four cases:

1. Non-sterilized sample sterilization:
  - a. Sample oriented with axis parallel with building direction ( $z$  axis).
  - b. Sample oriented with axis perpendicular with building direction ( $z$  axis).
2. Sterilized sample:
  - c. Sample oriented with axis parallel with building direction ( $z$  axis).
  - d. Sample oriented with axis perpendicular with building direction ( $z$  axis).

As mentioned, in the literature values for compressive strength of sterilized part could not be found. However, there are references to researches in which the compressive strength of ABS part is measured for raster angles of  $45^\circ$  (as is also the case of our samples).

For instance, Zieman et al. [18] reports a value of 24.46 MPa for the compressive strength, Wu et al. [19] reports a value of 28.4 MPa for samples built with axis along  $z$  axis. Ahn [10] reports a value of 27 MPa for samples built with axis parallel with  $z$  axis and 30 MPa when cylinder axis is perpendicular to  $z$  axis. Thus, the values determined in our tests correspond to the value reported in literature.

In Fig. 10 the yield stress variations for the two ABS samples, perpendicular and parallel to  $z$  axis, sterilized versus non-sterilized are presented. It can be observed that for parallel-sterilized specimens a significant increase of yielded stress occurs, but with minor geometrically modifications, while for perpendicular sample the yielded stress remains almost at the same value. This can be explained by the fact sterilization (heating at  $60^\circ$  followed by cooling at room temperature) is like a treatment process, removing tension from the part and improving its compressive strength.

Thus, if possible, according to the experiment results of this paper, the manufacturing recommendation is to orient the part so that to be built with the zones subjected to compression during use, perpendicular to  $z$  axis building direction.

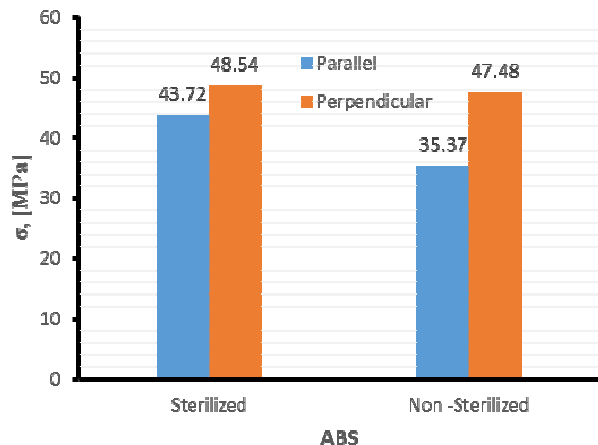


Fig. 10. Variation of yield stress.

Table 2

Some of the measured values for the test part, before and after sterilization process

Feature	Nominal value	Before sterilization	Deviation %	After sterilization	Deviation %
Slots – set 1 (N) (along $x$ axis)	1.37	1.151	15.98	1.418	-3.5
	1.37	1.161	15.25	1.406	-2.63
	1.37	1.147	16.27	1.385	-1.09
	1.37	1.133	17.3	1.37	0
Holes – set 1 (G) (along $x$ axis)	0.75	0.561	25.2	0.746	0.53
	1	0.819	18.1	0.958	4.2
	1.25	1.096	12.32	1.212	3.04
	1.5	1.365	9	1.469	2.07
Holes – set 2 (G) (along $y$ axis)	0.75	0.577	23.07	0.68	9.33
	1	0.791	20.9	0.944	5.6
	1.25	1.067	14.64	1.207	3.44
	1.5	1.335	11	1.454	3.07
Slots (F) (along $x$ axis) along $y$ axis	1.27	1.32	-3.94	1.26	0.788
	1.27	1.34	-5.51	1.243	2.12

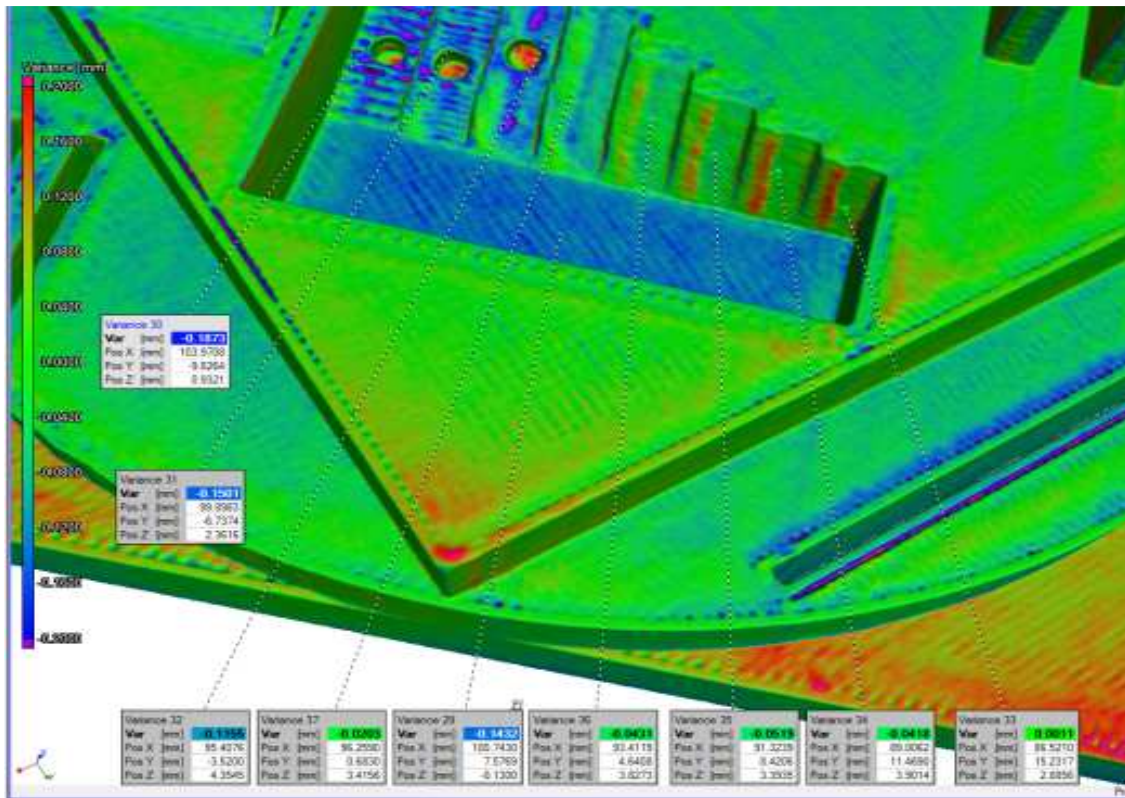


Fig. 11. Deviation color map for the pocket zone of the sterilized test part.

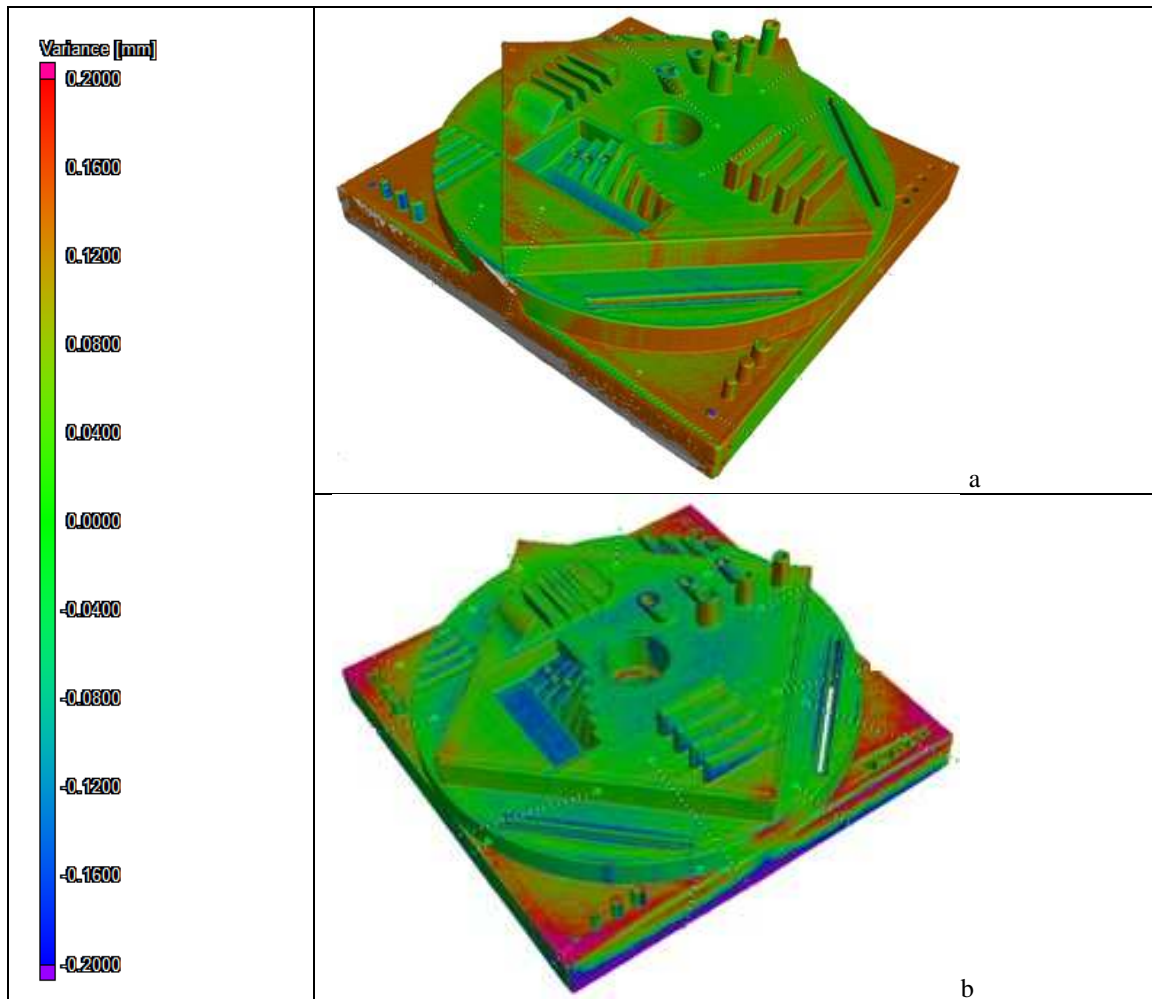


Fig. 12. Deviation map manufactured test part-nominal test part:  
 a – test part before sterilization; b – test part after sterilization.

**Dimensional accuracy.** After manufacturing, several dimensions of the ABS test part were measured and compared to the nominal values in different sections. A virtual test part was reconstructed based on the physical test part and deviation values were calculated. Figure 12,a shows the color map ( $\pm 0.27$ mm) for the test part before sterilization, while in Table 2, column 3 some of the measured values are presented. The color map for the non-sterilized test part showed mostly positive deviations in comparison with the nominal part.

The second measurement process was performed on the same test part, but this time after low-temperature sterilization process (Fig. 12,b). The color map is smaller  $\pm 0.20$  mm showing that the sterilized part dimensions are closer to the nominal part in comparison with the case when the part was not sterilized. Table 2, column 4, presents some of the measured values from the sterilized part (slots, holes). During the post-processing part for support structure removal, the 0.75 mm diameter pins broke and therefore they could not be measured.

For the non-sterilized part, the largest negative deviations of the nominal part were measured on the bottom horizontal plane surface of the pocket M (see Fig. 1 and Table 1). The horizontal surfaces of the parallelepiped base were built with positive deviation values up to 0.11 mm. For the sterilized part (Fig. 11), the largest deviations were noticed on the same pocket, but also on the inclined hollow cylinders. Positive variations were noticed on the plane surface of the parallelepiped base.

Figure 12 shows comparative color maps for sterilized and non-sterilized test part. At the corners of the parallelepiped base, the deviation values are maximum negative in comparison to the nominal part. However, in general, the sterilized part has dimensions closer to the nominal part.

## 5. CONCLUSIONS AND FURTHER WORK

Several conclusions can be drawn from the experiments presented in the current paper:

- Mojo 3D Printer can ensure a dimensional accuracy suitable for manufacturing surgical guides.
- Test part geometrical features dimensions proved to be sterilization-stable.
- No significant shrinkage was noticed on the test part; therefore sterilization would not negatively affect surgical accuracy of guides.
- Sterilization process improves the compressive strength of the test part.

Further testing will consider the use of at least five objects/samples of the same type for improving result confidence by considering measurement repeatability and reliability. Moreover, further work will be focused on comparative assessing of both compressive and tensile strength of parts manufactured using FDM process using other materials such as ULTEM, PLA (Polylactic acid) or PA 12 (Polyamide), also in two building orientations.

**ACKNOWLEDGEMENTS:** The work was funded by the Partnerships in Priority Areas Programme – PN II of MEN – UEFISCDI, through Agreement 5/2014.

## REFERENCES

- [1] C.L. Ventolla, *Medical applications for 3D Printing: Current and Projected Uses*, Pharmacology and Therapeutics, vol. 39, no. 10, 2014, pp. 704–711.
- [2] S. Bose, et al. *Bone tissue engineering using 3D printing*, Materials Today, vol.16, no. 12, 2013, pp.496-504
- [3] J. Chimento, et al., *3D printed tooling for thermoforming of medical devices*, Rapid Prototyping Journal, vol. 17, no.5, 2011, pp. 387–392.
- [4] H.H. Malik, A.R. Darwood, et al. *Three-dimensional printing in surgery: a review of current surgical applications*, J. Surg Res. Vol. 199, no. 2, 2015, pp. 512–522.
- [5] Stratasys White Paper, *Advancing Health Care With 3D Printing. Applications and guidance on material selection*, 2015, available at: <http://www.stratasys.com/resources/white-papers>.
- [6] M. Anton, *Performance 3D Printing with FDM Material*, Stratasys White Paper, 2014, available at: [www.cinteg.de](http://www.cinteg.de).
- [7] M. Perez et al. *Sterilization of FDM-manufactured parts*, Twenty-third Annual International Solid Freeform Fabrication Symposium – An Additive Manufacturing Conference, 6-8 August 2011. Austin, TX.
- [8] R.Y. Neches, et al. *On the intrinsic sterility of 3D printing*, Peer J PrePrints 2, 2014, issue e542v1 <https://doi.org/10.7287/peerj.preprints.542v1>.
- [9] P. Fünstahl, S. Wirth, L. Nagy, A. Schweizer. *Advantages and pitfalls in computer assisted orthopedic surgery using rapid-prototyped guides*. RTEjournal - Forum für Rapid Technologie, 2014, vol. 11, no. 1, available at: <https://www.rtejournal.de/ausgabe11/3946>.
- [10] S. Ahn, et al. *Anisotropic material properties of fused deposition modeling ABS*, Rapid Prototyping Journal, 2002, vol. 8, no. 4, pp. 248–257.
- [11] A. Bagsik, et al. *Mechanical properties of Fused Deposition Modeling parts manufactured with ULTEM\*9085*, ANTEC, Boston, 1–5 May, 2011.
- [12] M.S Hossain, et al. *Improving Tensile Mechanical Properties of FDM-Manufactured Specimens via Modifying Build Parameters*, Solid Freeform Fabrication Symposium, Austin Texas, 2013, pp.380–392.
- [13] A.K.Sood et al. *Parametric appraisal of mechanical property of Fused Deposition Modeling processed parts*. Mater Design, 2010, vol. 31, pp. 287–295.
- [14] S. P. Moylan, et al. *An Additive Manufacturing Test Artifact*. J Res Natl Inst Stand Technol. 2014, vol. 119, pp. 429–459.
- [15] M. Mahesh, et al. *Benchmarking for comparative evaluation of RP systems and processes*, Rapid Prototyping Journal, vol. 10, no. 2, 2004, pp.123–135.
- [16] L. Yang, et al. *An investigation of standard test part design for additive manufacturing*, Solid Freeform Fabrication Symposium, Austin Texas, 2014, pp. 901–922.
- [17] D. Popescu, D. Laptoiu. *Rapid prototyping for patient-specific surgical orthopaedics guides: A systematic literature review*. Proceedings of the Institution of Mechanical Engineers, Part H: Journal of Engineering in Medicine, vol. 230, no. 6, 2016, pp. 495–515.
- [18] C. Ziemian, M. Sharma, S. Ziemian, *Anisotropic Mechanical Properties of ABS Parts Fabricated by Fused Deposition Modelling*, Mechanical Engineering, Dr. Murat Gokcek (Ed.), 2012, available at <http://cdn.intechopen.com/pdfs-wm/35261.pdf>.
- [19] W. Wu, et al. *Influence of Layer Thickness and Raster Angle on the Mechanical Properties of 3D-Printed PEEK and a Comparative Mechanical Study between PEEK and ABS*, Materials, vol. 8, 2015, pp. 5834–5846.